TRI-SERVICE 2007
CORROSION CONFERENCE
ARMY • NAVY • AIR FORCE • MARINES • COAST GUARD • NASA

SENSORS FOR MEASUREMENT OF CORROSION RATES AND DETECTION OF CORROSION UNDER COATINGS

Ashok Kumar
L. D. Stephenson
Jeremy Hale
U. S. Army Engineer research & Development Center (ERDC)
Construction Engineering Research laboratory (CERL)
P. O. Box 9005
Champaign, IL 61826-9005

and
John Murray
Murray's et. al.
Timonium, MD

ABSTRACT

Corrosion rate measurement can reveal which areas of a structure need immediate maintenance and which ones will need maintenance later, as well as allow an optimal maintenance schedule to be developed. A new stamp-sized corrosion sensor allows measurement of corrosion rates based on well-established LPR (Linear Polarization Resistor) technology, which outputs an exact corrosion rate for the structure on which it is placed. The corrosion rate data can be monitored continuously or stored in a data collection node, to which 8 sensors are attached, and downloaded periodically. This sensor technology is being evaluated in the laboratory under various simulated corrosive field conditions. The sensor is being considered for corrosion monitoring applications on structures for mission critical equipment on military installations in severely corrosive environments. Results of laboratory experiments on the sensitivity of the sensor to the onset of corrosion on the substrate and projections for its applicability in the field will be discussed.

INTRODUCTION

Innovative remote sensors can provide data on corrosion status at various locations of mission-critical metal structures. The sensors can be applied to surfaces of mission-critical steel structures, and will respond to intrusion of moisture, which causes decreased electrical resistance as they are affected by changes in the local corrosive environment. Corrosion rates can be predicted from the shifts in polarization resistance. Increasing corrosion rates signal the need for corrective action, such as removal of corrosion, and re-coating of the structure. The sensor to be employed is built on well-established

Linear Polarization Resistor (LPR) technology and is intended to output an exact corrosion rate for the structure on which it is placed. The sensor can be placed onto a structure that is stripped down to bare metal and then recoated, or on top of existing coatings that need to be over-coated. Based on this data, it can then be determined at what rate these surfaces are corroding.

Figure 1 shows the sensor at a magnification of 2X, comprised of interdigitated steel fingers on top of a polyimide support film. Starting with the untested but electrically shorted, sensor (No. 3), a typical plan view is presented as Figure II where three different sets of stripes can be seen, the gray areas being the top surfaces of the sensor, interdigitated steel 'fingers' (F), and the yellow-brown areas being the exposed top surface of the adhesive/polyimide support polymer (P). The width of the 'fingers is quite close to that stated by the supplier, namely the narrower 'active' finger being 145 μm (6 mils) wide and the counter/reference finger width being 460 μm (18 mils). The upper plane separation between the fingers ranges from 170 to 185 μm (6.5 to 7 mils). The exposed polyimide widths ranged from 65 to 75 μm.

EXPERIMENTAL PROCEDURES

Three uncoated LPR sensors had been previously provided, gratis, by the manufacturer for evaluation using EIS as the principal interrogation technique. Following four wet/dry cycles with the two 'good' sensors, all three were evaluated for the physical appearances of the various surfaces and dimensions of the sensors using an imaging system[2]. Plan and 3-D views, as well as a limited dimensional analysis of 'shorted' No. 3 sensor and the two environmentally characterized (Nos. 1 and 2) resulted in a rethinking regarding the previously held view of the sensor functionality. The comments regarding the physical appearances of the sensors are being made with limited discussions with the supplier and therefore may be modified at a later date.

A preliminary summary report[1] concluded: a) the three sensors yielded quite different Electrochemical Impedance Spectroscopy (EIS) spectra and responses to changes in the relative humidity (RH) of the 'test air', b) one of the sensors (No. 3) exhibited an electrical 'short circuit' response, c) the low frequency impedance values of the remaining two sensors in a dry environment were considerably higher than the previously determined results generated using the LPR measurement and analysis system and d) further experimental testing of the two 'good' sensors was required.

The two 'good', uncoated, sensors were exposed to three levels of relative humidity for normally one week followed by heatless drying by exposure in a closed vessel containing 'molecular sieves'. This drying approach had been previously used to completely dehydrate various engineering polymers without subjecting the polymers to excursions into the glass transition temperature range, thus assuring the polymer(s) remain in the 'as-received' condition. The electrochemical (EC) response to changes from 'dry' to 'wet' and vice versa was found to be quite rapid and suggests a surface water adsorption/desorption process controls the first-day, sensor condition and therefore the EIS data. The subsequent change in EC performance is then a function of water absorption within the polymer as well as the steel finger corrosion processes, then dependent on the level of relative humidity.
The EIS experiments were performed and involved 4 drying/wetting cycles as presented in Table 2. The sensors were positioned approximately 10 cm above the controlling environments. Complete dryness was attained with Type 13X molecular sieves beads. The 33 % RH condition was that over a saturated $MgCl_2 \bullet 6H_2O$ solution[3], 38 – 55 % RH was normal for the lab during the time-frame and the 100% RH condition was via commercially available distilled water.

Two topics are addressed below; the first is the documented surface examination of mainly Sensor #3, which had not been exposed to the cyclic humidity experiments but with some views included from the rusted sensors, Nos. 1 & 2. The second topic is a summary of the EIS testing.

RESULTS AND DISCUSSION

Physical Evaluation

The imaging system used for physical evaluation of the sensor combines digital 'photography' with microscope viewing of a sample positioned on a precisely controlled x,y,z table. After an initial plan view of the sample is recorded, the z-position is incrementally changed several times as defined by the analyst with only the in-focus information stored in the computer. The software then reassembles/overlays all the x-y data resulting in a 3-D 'reconstruction' of the object's 'surface'. This data file (or surface) can subsequently be rotated by the analyst. Section slices can be dimensionally analyzed as well as areas and surface volumes for data of particular interest.

Figure 1 is a schematic of the sensor, comprised of interdigitated steel fingers on top of a polyimide support film. Starting with the untested but electrically shorted, sensor (No. 3), a typical plan view is presented as Figure 2 where three different sets of stripes can be seen, the gray areas being the top surfaces of the sensor, interdigitated steel 'fingers' (F), and the yellow-brown areas being the exposed top surface of the adhesive/polyimide support polymer (P). The width of the 'fingers is quite close to that stated by the supplier, namely the narrower 'active' finger being 145 μm (6 mils) wide and the counter/reference finger width being 460 μm (18 mils). The upper plane separation between the fingers ranges from 170 to 185 μm (6.5 to 7 mils). The exposed polyimide widths ranged from 65 to 75 μm.

The upper surface of the steel fingers is seen to lay above the adhesive/polyimide surface and the steel finger sides are confirmed to be tapered. The image appears to be skewed and with the complete software, this can be corrected and 'made' planer. The demo software can come closer to showing the taper nature of the fingers. Two artifacts are apparent at the top edge of the wider finger and these were retained rather than removed.

The thickness of the steel was determined to be between 55 and 60 μm (2 – 2.1 mils) based on the section thickness profile feature of the imaging software and this value agrees with the thickness of the steel stated by the supplier. The general appearance indicates that the steel fingers are not permanently, significantly imbedded within the polymer. Whether the moisture absorption/desorption cycling for Sensors 2 & 1 contribute to a detachment of the steel from the polymer is not determined at this point. As the imaging system never "sees" the bottom plane of the polyamide floor, this thickness and any disbondings could not be documented.

In subsequent examinations, additional general features were seen. The upper metal finger surface showed what appeared to be polish or scratch lines running across the finger widths and roughly 6 rust areas were also evident on the counter/reference finger. Again the corrosion was most evident along the tapered sides of the fingers. The dimensional analysis from the plan view(s) is summarized in Table 1.

The appearance of Sensor 1 was somewhat distinct in that the taper sides oxide layer seemed more pronounced and 'organized'/dense. Also the scratch/polish lines seemed to be more pronounced. The

upper surface rust was evident and somewhat more spread out than seen with Sensor 2. The finger width dimensions are included in Table 1.

Previously, the supplier had stated that the metallic sensor fingers were imbedded into the polyimide base. As seen in Figure 2, clearly this is not the case. Following that non-destructive evaluation of the thickness of the steel fingers height(s) and width(s), during the subsequent QA/QC visit to the supplier, the sensor fabricator disclosed more of the fabrication process detail. Essentially, an approximately 25 μm thick layer of a high temperature melt adhesive is applied to one side of the 25 μm thick polyimide film. The 50 μm thick metal (in this case AISI 1010 steel shim stock) is then hot pressed onto the adhesive layer. The pattern for the steel fingers etc. is then established by photo engraving and leaching the unwanted metal, rinsing and finally drying the sensor element. Although not discussed, this might be accomplished by starting with a 50 μm thick adhesive layer. Following the metal removal and washing/drying step, it may be possible to re-hot-press the steel fingers, the adhesive then possibly flowing into the acid created channels, with temperature, pressure and time being the controls to stop the process when the adhesive 'just fills' the void.

Thus it appears that the actual configuration of the sensor is not as had previously envisioned. While this does not affect the sensor serving to activate when exposed to corroding conditions, questions as to the amount as well as location of active metal involved in the process do remain. Resolving those questions appears to be necessary to fabricate a set of sensors with reasonably close operating characteristics as well as to improve operation in combination with whatever limitations exist within the LPR measurement and analysis system. This should be accomplished by implementing a quality control procedure to insure that the actual configuration of the LPR sensor is in accordance with the original design, i.e., that the fingers of the sensor are embedded in the polyimide film.

EIS and Moisture Cycling of the Sensors

As discussed previously[1], the EIS data from the two uncoated functional sensors were distinct with Sensor #1 having a low frequency impedance limit of approximately $1 \times 10^{12}\ \Omega$ compared to that seen for #2 of $4.2 \times 10^{9}\Omega$. The wetting and drying segments were performed on both sensors within the same test vessel. However, for brevity, as both sensors responded in the same general fashion the discussion will be limited to the 'behavior' of Sensor #2.

The EIS response for a change from dryness to the 33% RH condition is shown as Figure 3a. where the low frequency impedance drop from $3.1 \times 10^{10}\ \Omega$ to $7.3 \times 10^{9}\ \Omega$ is seen to occur within 6 minutes. The impedance magnitude decreased 50% over the following 7 days. The sensor basic capacitance did increase very slightly during the week as expected, the increase attributable to an increase in absorbed water from 0.24 to 0.6 v/o (volume percent). Although the low frequency range of the Bode Magnitude plot might be suggestive of the development of a second time constant, the Phase Angle plot does not support that notion as can be seen in Figure 3b taken at 1 week exposure.

A more dramatic initial (6 minute) drop of impedance during the dried sensor exposure to the lab ambient 53% RH is seen in Figure 4. Here the decrease was from $5.7 \times 10^{10}\ \Omega$ to $2.7 \times 10^{9}\ \Omega$. Again a small increase is observed in the sensor capacitance and attributable to the absorbed water rise from 0.6 v/o to 0.93 v/o. The EIS model also remained as a one time-constant model, this also being verified with the phase shift information.

There were two 100% RH environment exposures made, the first having been presented previously[1]. There, the drop in impedance in 6 minutes exposure decreased from roughly 4 x 10^9 Ω to 10^7 Ω and the impedance data were "two time-constant" type response. As indicated in Table 2, the second 100% RH exposure came as Segment 11, the 4th (and last) wet/dry cycle. The impedance data (Figure 5) dropped down to 2 x 10^4 Ω. In addition to seeing 'rust' on about 50% of the bare upper metal finger surfaces and on 90+ % of the finger electrical feeder strips, rust on the finger undersides and distortions to the polyimide indicate that considerably more than the upper metal surface was electrochemically active. Whether this additional corrosion "is" the cause of the 2nd time constant remains to be demonstrated.

The one week exposure, impedance data from the uncoated Sensor #2 are summarized as a function of the test RH as Figure 6. Included in the figure are two limit lines showing the current operating range for the LPR measurement and analysis system. The limits assume that the LPR measurements correspond to the low frequency EIS values, due to the relatively slow speed at which the LPR measurements are taken. The small decrease of the high impedance value of the uncoated steel sensor exposed to indoor exposures to between "0" and 50% RH is in agreement with many previous atmospheric corrosion studies and common experience. For example, detergent washed, towel dried, carbon steel knives remain rustless in conventional kitchens for very long periods of time.

In Mattsson's classical review[4] which covered the basics regarding atmospheric corrosion, he notes that (water) "adsorption occurs above a certain relative humidity, called the critical relative humidity." He gives no specific value for the 'critical RH" but does note that the amount of water that does absorb increases by 100 fold from that point to 100% RH. The ensuing problems that occur outdoors following water absorption are discussed for the 4 common metals (steel, zinc, copper and aluminum). Considerable additional detail regarding the atmospheric corrosion mechanism(s) for iron and steel are provided by Graedel and Frankenthal[5]. They repeat Mattsson's comment regarding a critical level of RH and add that at 60% RH, an equivalent of two monolayers are on an iron/steel surface, but much in clusters rather than as a uniform layer.

Using the (then) newly available quartz microbalance, which can detect as low as approximately 1/3 of a water monolayer adsorbing onto a gold surfaced quartz crystal, Dante and Kelly[6] present water adsorption data. Starting from 4 water 'monolayers' on gold at 15% RH, the water thickens to 10 'monolayers' at 50% RH and approximately 43 'monolayers' at 85% RH. For gold, which does not react at room temperature under normal conditions, the adsorption and desorption steps were quite rapid and reproducible, this being seen here with the uncoated steel sensor. Roughly 70 % of the crystal response occurred within 5 minutes after a step from 15% to 85% RH or vice versa. Lee and Staehle[7] repeated the gold/quartz microbalance study, evaluating the effects of RH in the experimental temperature range from 7 to 90 C. Their results were similar to the Dante results with however, the significant increase in absorbed water occurring more towards the 70% RH level. Their data also show the desorption rate to be about 3 times faster than the adsorption rate. The effort was expanded to include iron[8] as well as copper and nickel. The complexities of having a surface (Fe) that can electro-oxidize without oxygen present and the influence of the oxide film(s) on the adsorption characteristics are presented. Their data suggest that the least amount of water was adsorbed on the iron surface, although the applied surface roughness 'correction' may not have been as rigorous as one would like. The response of the LPR sensor is consistent with these results, as it exhibits a slow decrease in impedance magnitude with increasing RH and then a much more rapid decrease in impedance magnitude as the RH (and thus the adsorbed moisture) increases beyond 50% upwards to 100%.

Sensors on Glass Plates

Painted Sensor Drying. Four linear polarization resistance sensors from the supplier were adhered to two glass plates by epoxy 5 cm (2 in.) from each other. Two of these linear polarization resistance sensors were then coated with two coats of Sherwin Williams B73 W111/V100 paint and allowed to dry. Two similar sensors were coated with three coats of the same paint and also allowed to dry. Using the LPR measurement and analysis system from the supplier, corrosion rates were monitored over the course of three weeks along with relative ambient humidity in the laboratory space. This three-week period began with painting the sensors with the first coat of paint, followed by a second coat a week later, and a final coat of paint was applied to the sensors in the third week. Measurements during the drying time of all sensors appeared be above the upper limit of the LPR measurement and analysis system. All data points from every sensor registered at 7.5×10^7 ohms.

Humidity Exposure, The four sensors attached to two glass plates were then suspended 10 cm (4 in.) over an enclosed trough of water while readings were taken by the LPR measurement and analysis system. After two weeks of measurement, a scratch was cut 0.84 cm (0.33 in.) away from one sensor and 4.22cm (1.66 in.) away from the other on each plate (See Fig 7). The sensors were then placed back over the water bath for two more weeks. Measurements were taken during this time. Measurements were again at a consistent maximum of 7.5×10^7 ohms even with the consistent 100% humidity. Scribing the paint did not make any difference in any readings of the sensors.

UV/salt fog exposure. The remaining LPR sensors were adhered by epoxy to specifically designed glass slides the correct dimensions to insert into UV/Salt Fog ASTM D 5894 Test. Over the course of 12 weeks the sensors will be monitored every 10 minutes by LPR measurement and analysis system. This experiment is still currently underway. Due to the harsh nature of the test and its duration, measurable results are expected.

Sensors on Glass Plates UV/CON Exposure. Finally, three LPR sensors were adhered by epoxy to specifically designed glass slides the correct dimensions to insert into UV/CON ASTM D 4587-05 Test Standard Practice for Fluorescent UV-Condensation Exposures of Paint and Related Coatings. Coated sensors were tested over the course of 12 weeks the corrosion rates were recorded every 10 minutes. Figure 8 shows some of the panels with the sensors under the coating. The UV/CON exposure simulated corrosion rate under coating due to coating degradation for cycles of 4hr. UV @ 60 deg F followed by 4 hr Condensation @ 40 deg F.

The results are shown in Figure 9a , 9b, and 9c. It is seen that the corrosion rate follows the wet and dry cycles for all 3 LPR sensors, consistently through out the 12 weeks, with a slight lag at the beginning of both the wet and dry cycles in the first week, but tracking the onset of wet and dry cycles without delay by the 6^{th} week. .It is also seen that the maximum corrosion rate decreased consistently throughout the test. The interpretation of these somewhat surprising results were that the paint had performed well as a corrosion barrier and was in the process of "drying out" as it cured over time and UV exposure. Note that the corrosion rate, which initially showed initial corrosion rates at 10^{-3} mm/yr had stabilized to 8×10^{-5} mm/yr. by the 12^{th} week of UV/condensation exposure. Laboratory tests are continuing to determine if the sensors will show higher corrosion rates eventually if the paint is subjected to more cycles of UV. Also, similar LPR sensors have recently been installed under water-born epoxy paint on a metal roof at an Army Installation in Okinawa, Japan, in a severely corrosive coastal environment located within 1 km from the ocean. The corrosion rate data will be measured at

15 minute intervals and transmitted remotely to our laboratories to determine long term field performance of the sensors over the next year.

CONCLUSIONS

The uncoated steel (LPR) corrosion sensor shows an expected low frequency impedance response as a function of exposure to the RH. The high impedances seen at low RH values via the EIS system are considerable higher than the measuring capability of the LPR measurement and analysis system. At the high humidity ranges, the LPR measurement and analysis system can measure LPR values as low as $2.5 \times 10^4\ \Omega$, which for a steel sensor, may be approaching the higher corrosion current measuring limits. While this may be unsatisfactory to some who prefer more complete knowledge regarding the state of steel in a potentially corroding environment, the fact that the LPR measurement and analysis system provides "safe" vs. "unsafe" condition 'measurement' may be sufficient. This limited study also showed two additional problems. The widely different electrochemical response of these three manufactured sensors is obviously a QA/QC problem. An independent evaluation of a set of at least 8 sensors is warranted to see the response spread of the current manufacturing variances. And although not discussed, but perhaps observable from the drop in impedance via the EIS data and post test visual examinations, the sensor deterioration during or following the 4^{th} moisture adsorb/desorb cycle may be indicative of a disbonding of the steel 'fingers' from the adhesive. This potential problem may be resolved if the sensor manufacturer can 'truly' imbed the fingers within the polymer layer.

Conclusions for the first two experiments, viz., EIS/moisture cycling and humidity exposure are that there was either no degradation of the sensor due to corrosion or, more likely, the upper limit on the LPR measurement and analysis system is set too low.

From the UV/CON experiments, it was concluded that the coated glass plated subjected to UV/CON to simulate measure of corrosion rate under coating due to coating degradation at 4hr. UV @ 60 deg F/ 4 hr Condensation @ 40 deg F showed initial corrosion rates at 10-3 mm/yr. decreasing over a period of 6 weeks and then stabilizing to 8 X 10-5 mm/yr. Corrosion rates were consistent with UV/CON test cycles,: increasing with condensation (moisture laden environment) and decreasing with UV exposure. The investigation is on-going to determine if this is due to the curing of the paint. These LPR sensors are now being tested in the field, and are being interfaced with a system which will allow transmission of data via the internet using satellite uplink/downlink.

REFERENCES

1. Murray, J.N.; "Draft #1d; Preliminary Evaluation of 3 Analatom Corrosion Sensors", Letter report to ERDC-CERL-IL (L.D. Stephenson), 30 April 2006.

2. Keynote Lecture presented by Prof. Joseph Payer (Case Western Reserve University), CORROSION 2006, March 2006, San Diego, CA.

3. Klassen, R.D. and P.R. Roberge; Support Viewgraph Materials for "Technical Note: Measuring Corrosiveness with a Dual Galvanic/Surface Film Resistance Sensor", Corrosion, 62, No. 3, pp 195 – 198, March 2006.

4. Mattsson, E.; “Corrosion: An electrochemical problem”, ChemTech., 15, No. 4, pp 234-243, April 1985.

5. Graedel, T.E. and R.P. Frankenthal; “Corrosion Mechanisms for Iron and Low Alloy Steels Exposed to the Atmosphere”, J. ECS, 137, No. 8, pp 2385 – 2394, Aug. 1990.

6. Dante, J.F. and R.G. Kelly; The Evolution of the Adsorbed Solution Layer during Atmospheric Corrosion and Its Effects of the Corrosion Rate of Copper”, J. ECS, 140, No. 7, pp 1890 – 1898, July 1993.

7. Lee, S. and R.W. Staehle; “Adsorption of Water on Gold”, Corrosion, 52, No. 11, pp 843 – 852, Nov. 1996.

8. Lee, S. and R.W. Staehle; “Adsorption of Water on Copper, Nickel, and Iron”, Corrosion, 53, No. 1, pp 33 – 42, Jan. 1997.

TABLE 1

Width Dimensions of Steel Fingers and Exposed Adhesive/Polyimide (microns; (mils))

	Polyimide 'floor'	Working Finger	Polyimide 'floor'	Counter/Ref Finger	Polyimide 'floor'	Working Finger
Sensor 3*	75	145	75	460	75	NA
	(3)	(6)	(3)	(18)	(3)	"
(From Excel Software)	73	137	68	434	NM	NM
Sensor 2	NA	NA	NA	425	70	120
	"	"	"	(16.5)	(2.5)	(4.5)
Sensor 1	75	115	80	415	70	NA
	(3)	(4.5)	(3)	(16)	(2.5)	"

NA = Not Available in viewed segment
NM = Not measured
* no scale bar available; values averaged from 'finger' specs.

TABLE 2
Chronology of Sensors Runs

Segment #	Dry(D)/Wet(W)	RH(%)	Dates
1	-	~30	3/9 – 3/10
2	-	~30	3/10 – 3/11
3	D	0	3/11 – 3/23
4	W	100	3/23 – 4/18
5	D	38	4/18 – 4/28
6	D	0	4/28 – 6/5
7	W	53	6/5 – 6/13
8	D	0	6/13 – 7/12
9	W	33	7/12 – 7/19
10	D	0	7/19 – 7/26
11	W	100	7/27 - 8/3
12	D	0	8/3 - 8/4

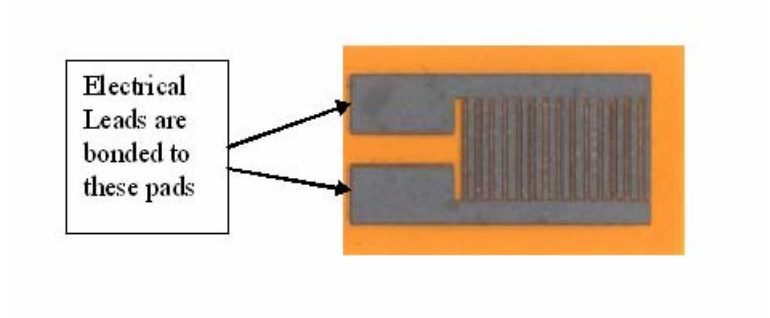

FIGURE 1 - Linear polarization sensor on polyimide film with interdigitated fingers (2X).

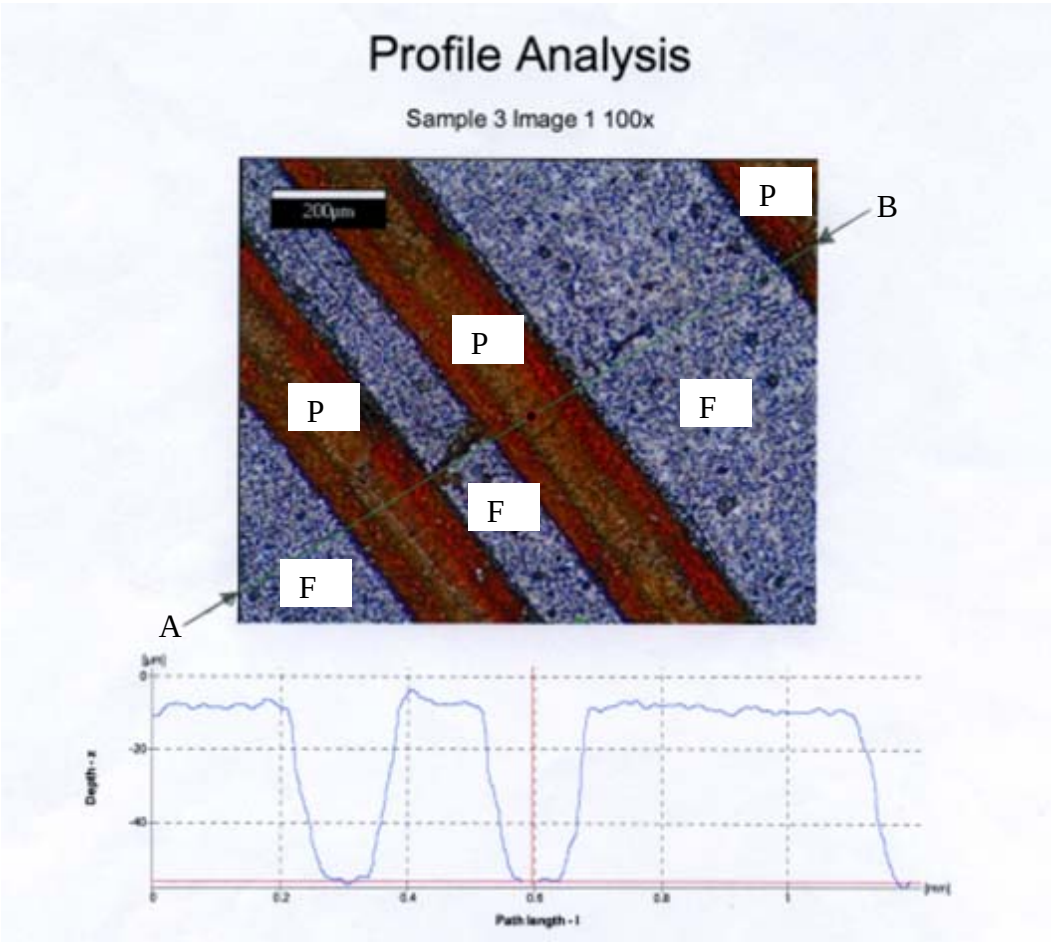

FIGURE 2 - Plan view of electrically shorted, sensor (No. 3), a typical plan view and profile along line AB (F- top surfaces of the sensor, interdigitated steel 'fingers'; P- exposed top surface of the polyimide support polymer).

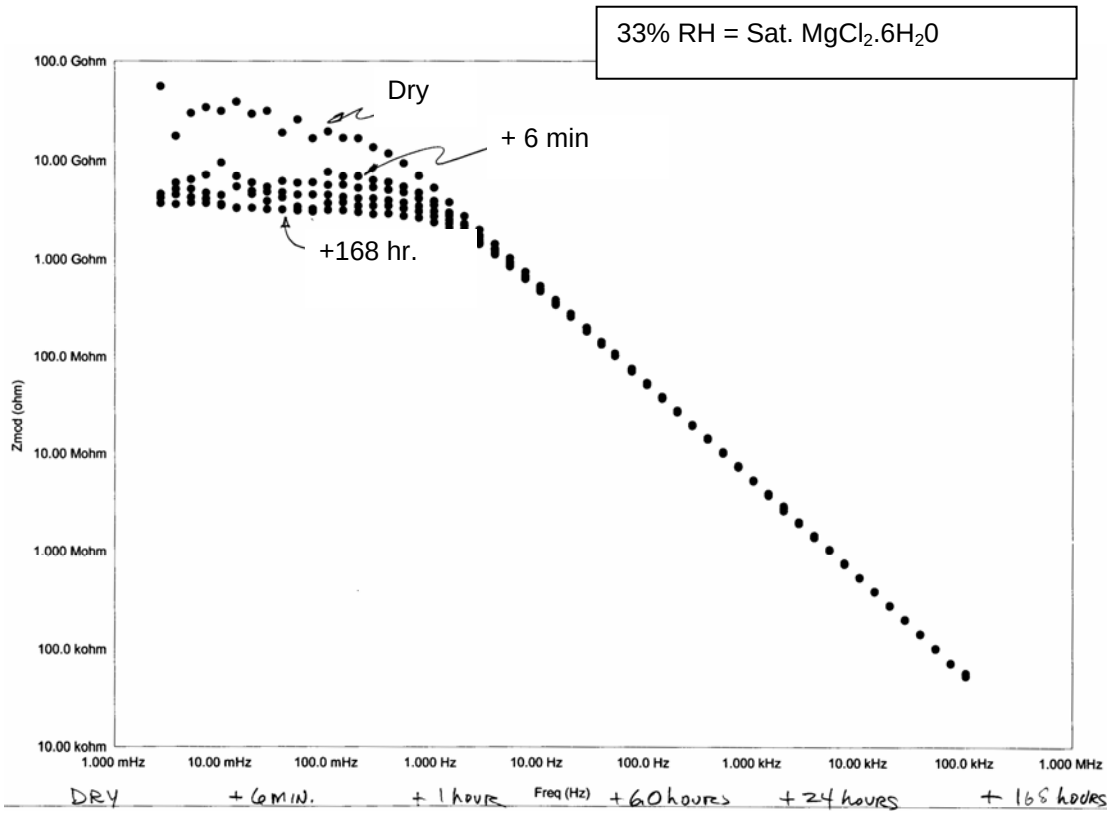

FIGURE 3a.- Sensor No. 2, EIS response(s), segment 9, 33% RH

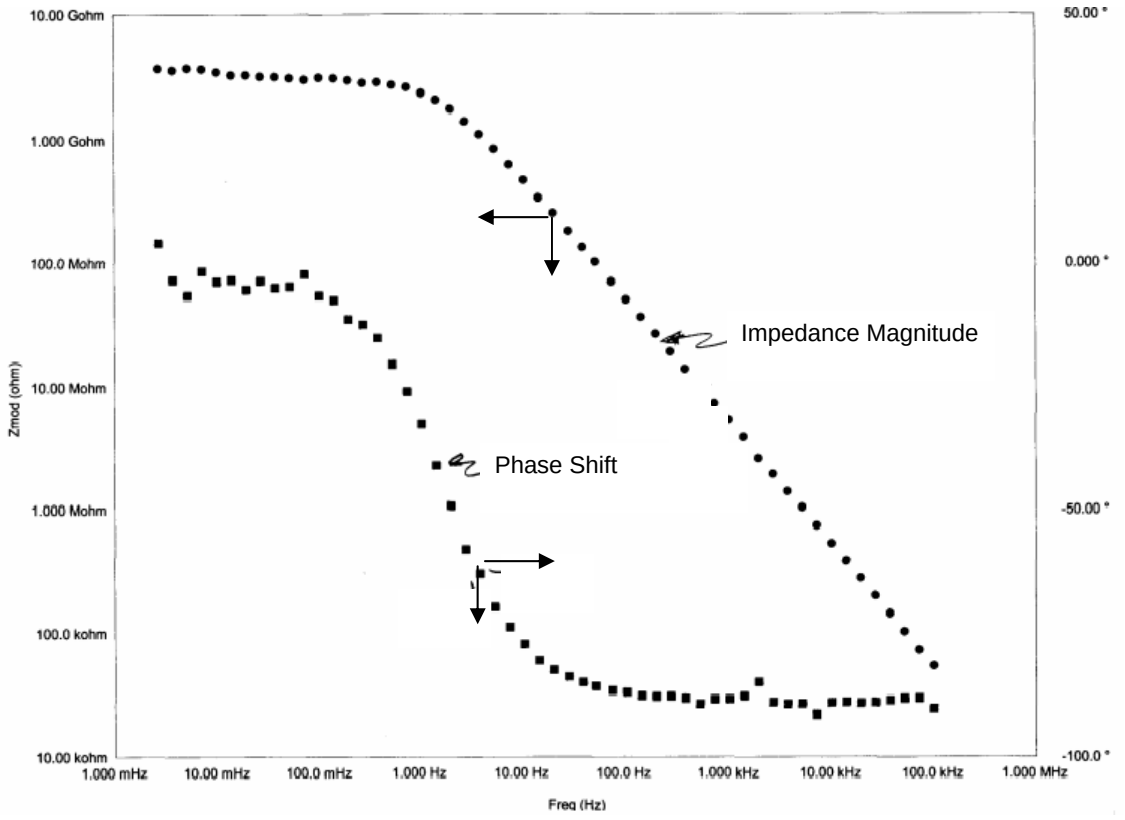

FIGURE 3b -. Sensor No. 2, EIS of 33% RH at 168 hours of exposure

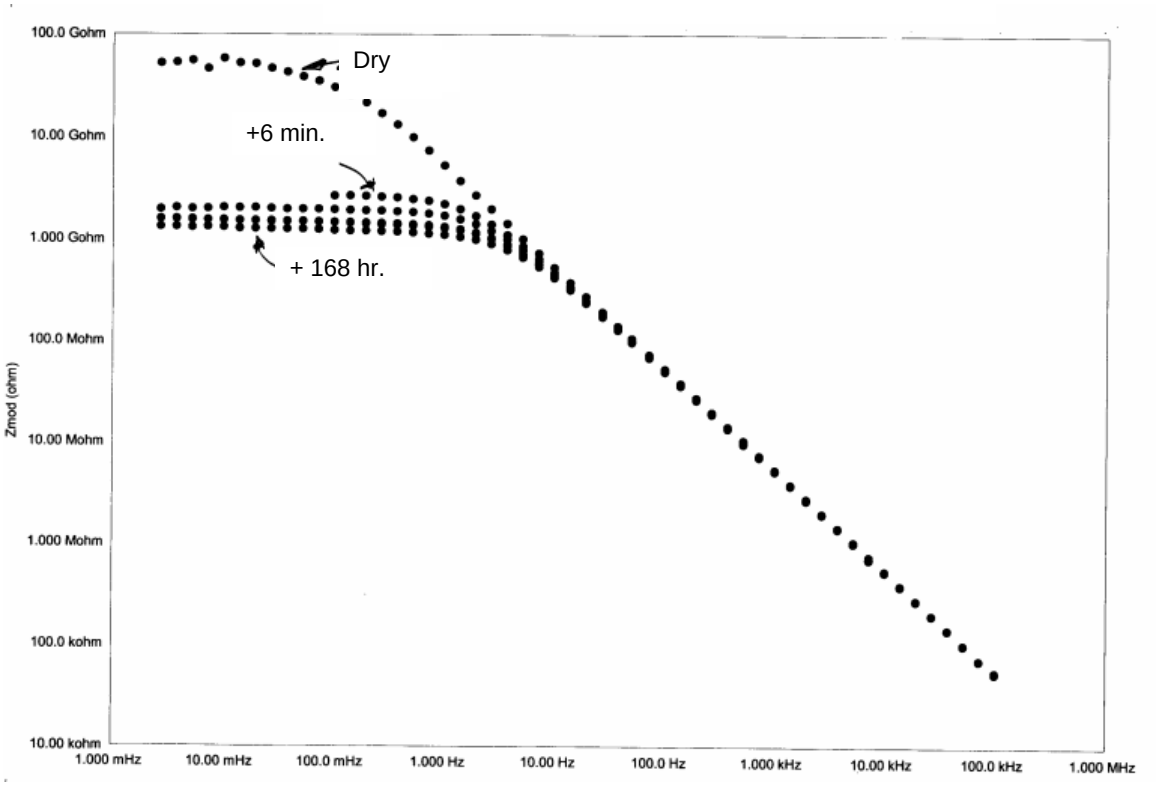

FIGURE 4 - EIS response (s), segment 7, 53% RH

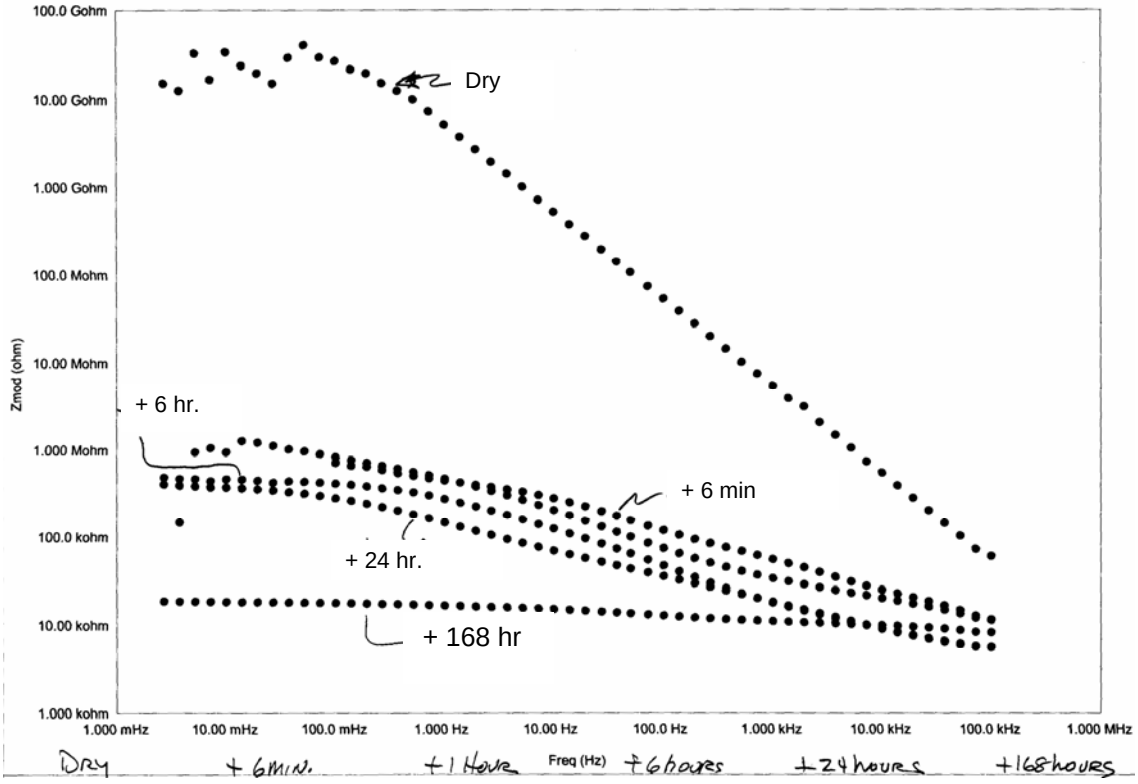

FIGURE 5 - Sensor No.2, EIS response(s), segment 11, 100% RH

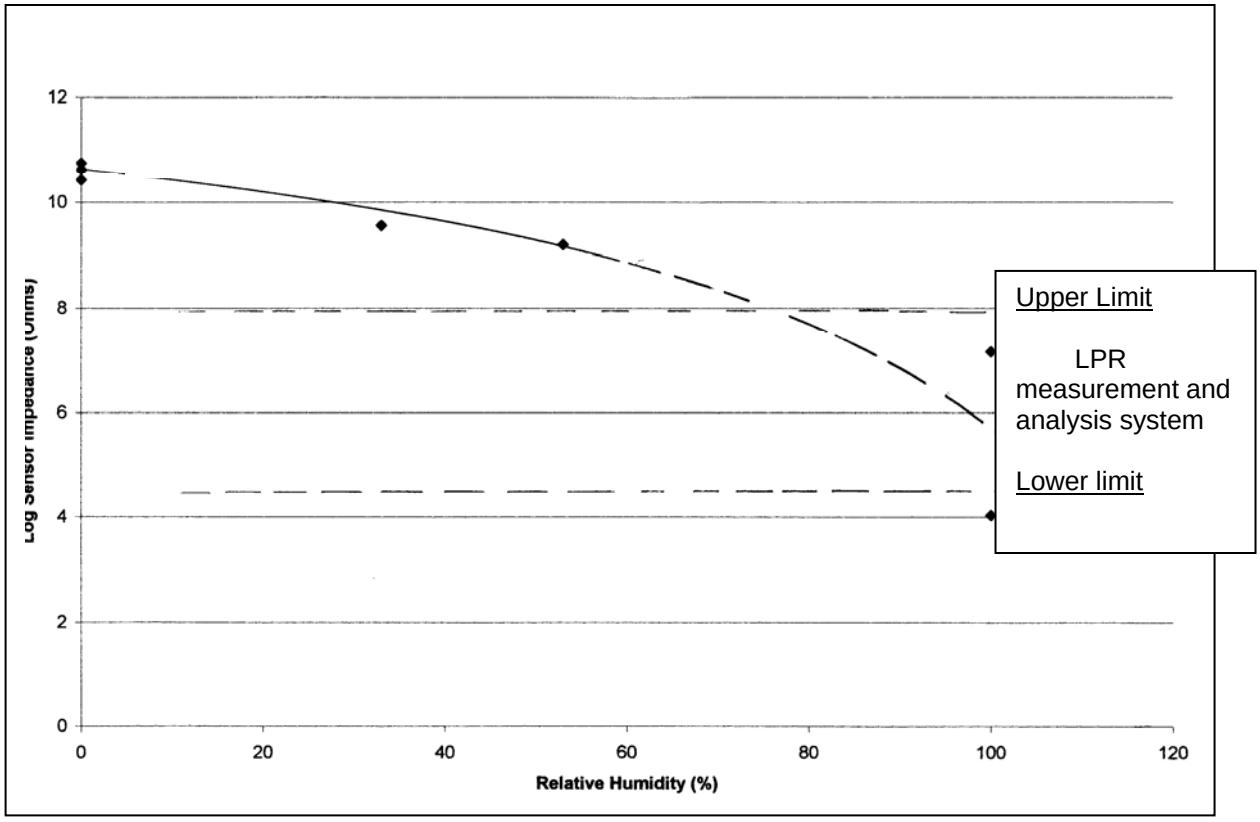

FIGURE 6 - Log sensor impedance vs. relative humidity

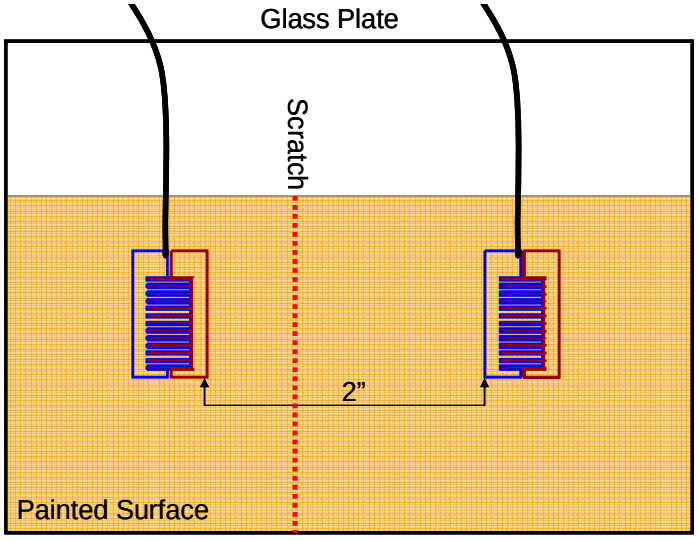

FIGURE 7 - Sensor set up on painted glass for 100% humidity and scribe testing.

FIGURE 8. Test panels consisting of water-borne epoxy coating painted over LPR sensors.

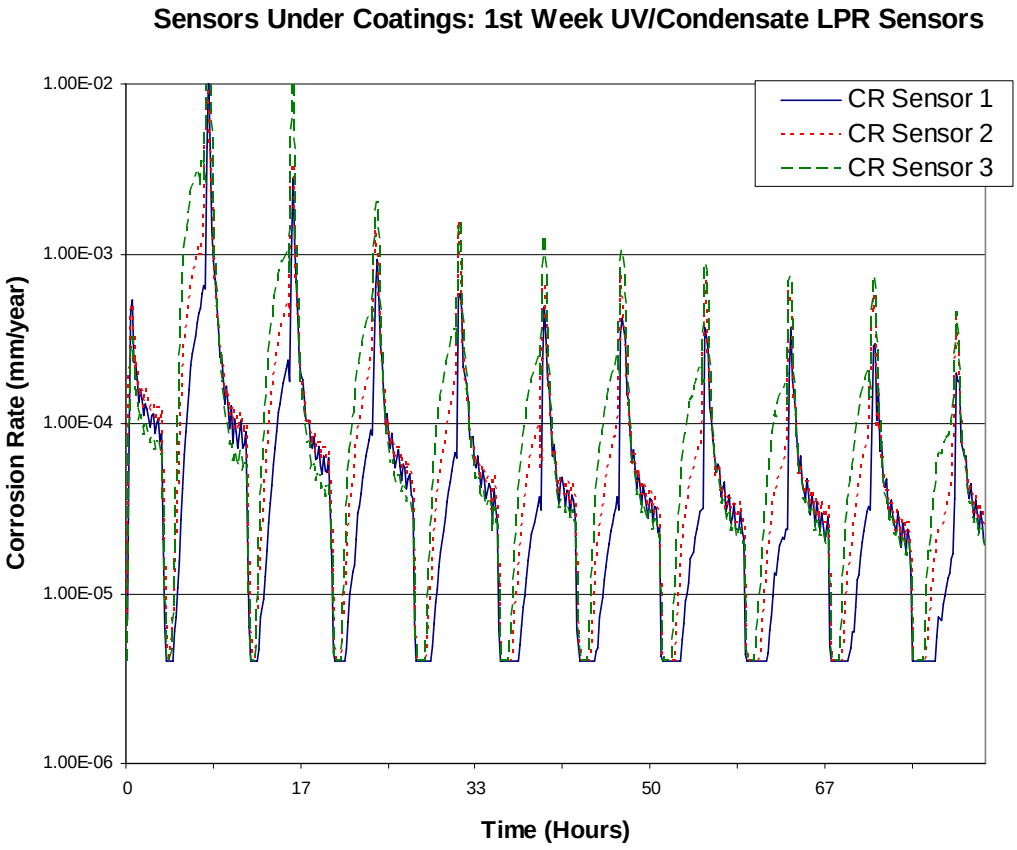

FIGURE 9 a. Corrosion Rate vs. Time for LPR sensor under paint subjected to UV/CON Exposure for 1 Week

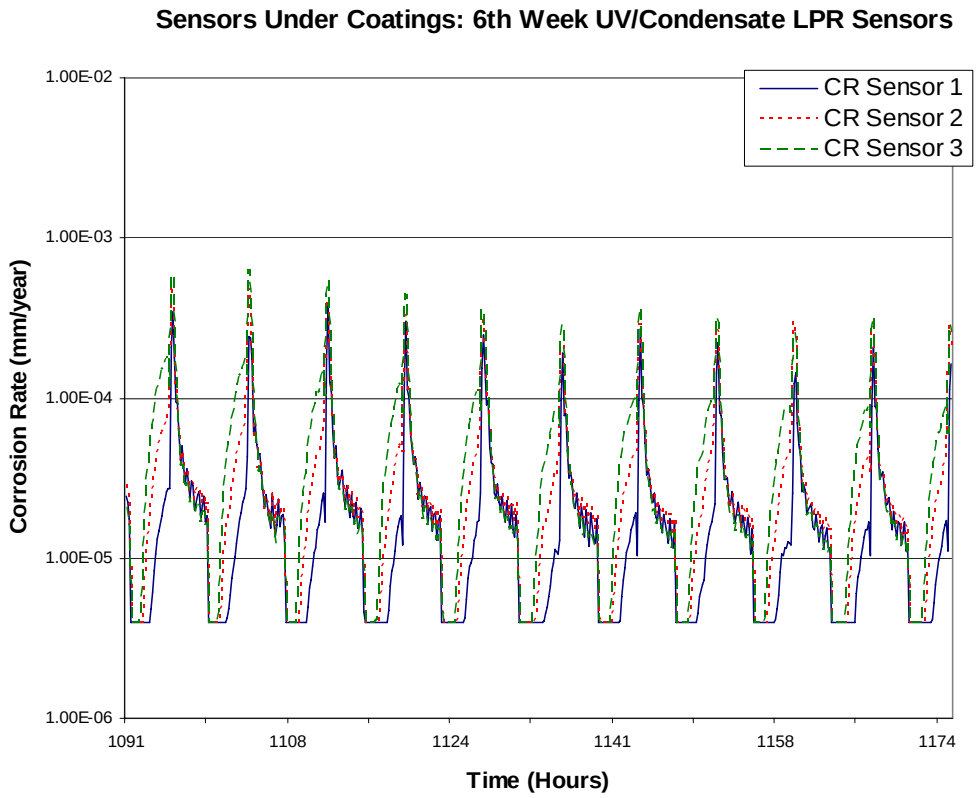

FIGURE 9b. Corrosion Rate vs. Time for LPR sensor under paint subjected to UV/CON Exposure for during Week 6.

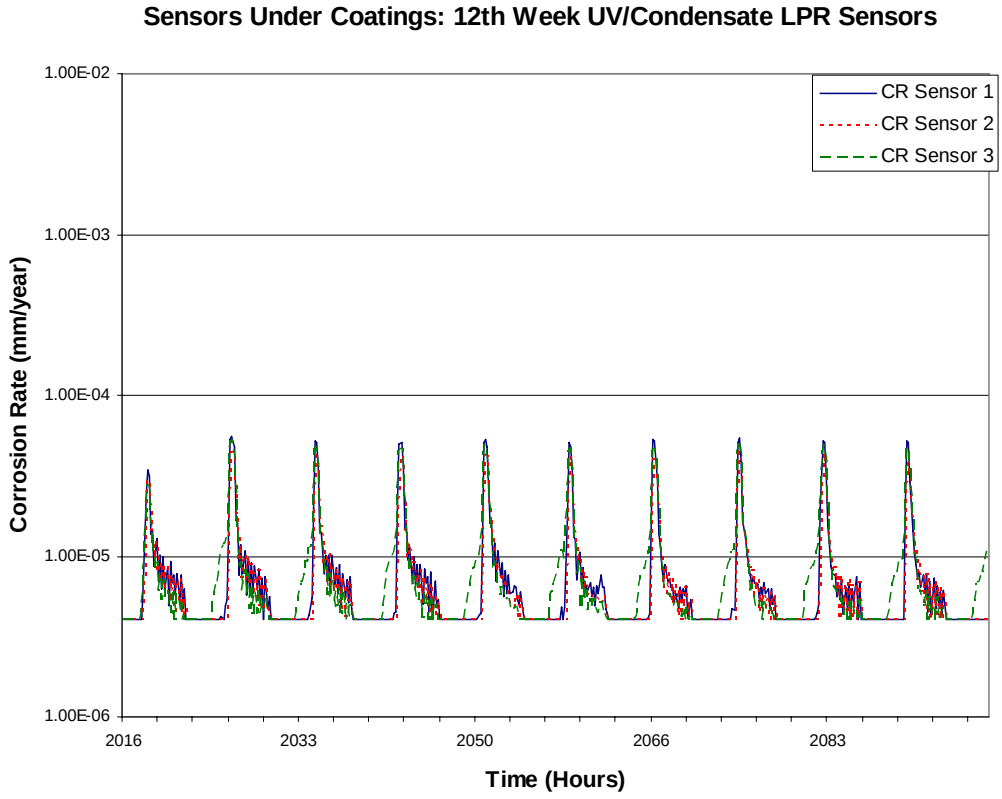

FIGURE 9c. Corrosion Rate vs. Time for LPR sensor under paint subjected to UV/CON Exposure for during Week 12.